Molecular Crystals and Liquid Crystals
Publication details, including instructions for authors and subscription information:
http://www.tandfonline.com/loi/gmcl20

Temperature and Wavelength Dependence of Effective Geometry Parameter and a Comparative Study of Orientational Order

Anant Kumar [a]
[a] Department of Material Science , University of Patras , Patras , Greece
Published online: 03 Oct 2013.

To cite this article: Anant Kumar (2013) Temperature and Wavelength Dependence of Effective Geometry Parameter and a Comparative Study of Orientational Order, Molecular Crystals and Liquid Crystals, 582:1, 43-55, DOI: 10.1080/15421406.2013.791964

To link to this article: http://dx.doi.org/10.1080/15421406.2013.791964

Mol. Cryst. Liq. Cryst., Vol. 582: pp. 43–55, 2013

ISSN: 1542-1406 print/1563-5287 online
DOI: 10.1080/15421406.2013.791964

Taylor & Francis
Taylor & Francis Group

Temperature and Wavelength Dependence of Effective Geometry Parameter and a Comparative Study of Orientational Order

ANANT KUMAR*

Department of Material Science, University of Patras, Patras, Greece

Temperature and wavelength dependence of effective geometry parameter, the ratio of ordinary and extraordinary refractive indices, is reported. A modified four-parameter model and the Cauchy equations are opted to explain the temperature and wavelength dependence of effective geometry parameter, respectively. Additionally, the order parameter variation of effective geometry parameter is also studied. Influence of effective geometry parameter on the deflection of light by the liquid crystal compounds is also discussed. Different methods for the determination of order parameter from the optical data are compared. The order parameter is determined by using the birefringence, Vuks, and Neugebauer methods. The fitting results, obtained by the application of four-parameter model and Cauchy equations, are validated using the experimental data available in literature. A fine agreement is obtained between the experimental data and fitting results.

Keywords: Effective geometry; nematic liquid crystals; orientational order; refractive indices

1. Introduction

Liquid crystals (LCs) have found wide commercial applications over the last few decades but the most common application is liquid crystals displays (LCDs). LCD technology requires detailed information about the liquid crystal materials, their response to external fields, and their optical properties. A nematic liquid crystal (NLC), due to its orientational order, behaves as an optically uniaxial crystal and its properties exhibit anisotropy [1, 2]. LC anisotropy covers a broad range of properties like viscosity, elasticity, birefringence, electric permittivity, magnetic susceptibility, etc. Among these properties, the optical birefringence is a crucial parameter from the application point of view [3–5]. Hence, it is essential to study the wavelength and temperature dependencies of LC refractive indices. The refractive indices of LCs are influenced by the molecular structure, operating temperature, and wavelength of light. Several theoretical models [6–10] have been developed to correlate the refractive indices of liquid crystals with the operating temperature and wavelength. Here, a modified four-parameter model [11] has been used to explain the temperature dependence of NLC refractive indices. The three coefficient Cauchy model [10] is applied to describe the wavelength dispersion of refractive indices. Fitting results obtained by the application

*Address correspondence to Anant Kumar, Department of Material Science, University of Patras, Patras 26504, Greece. E-mail: akumar@upatras.gr

of the four-parameter model and Cauchy equations are validated using the experimental data of four different nematics.

Topological defects are unavoidable results of continuous symmetry breaking phase transition [12]. In the bulk isotropic-nematic phase transition, an LC jumps from an ordinary liquid to an orientationally ordered configuration. In I-N transition, continuous symmetry breaking takes place. Topological defects in NLCs arise due to I-N phase transition [13]. In calamitic liquid crystals, these defects are found in the form of hedgehogs, disclination, domain walls, or other complicated textures [14, 15]. Topological defects cause the light passing through to deflect in a direction determined by the orientation of the director associated with the defect and the intensity of deflection depends on effective geometry parameter (α_{eg}), which is the ratio of ordinary (n_o) and extraordinary (n_e) refractive indices [15]. Thus, the knowledge of effective geometry parameter is important to understand the behavior of light propagating in LC compounds, particularly the effect of temperature and wavelength.

Satiro and Moraes [15] proposed that the effective geometry depends only on the parameter ($\alpha_{eg} = n_o/n_e$), which, in turn, depends on the temperature and wavelength of light. They have used α_{eg} to explain the propagation of light near disclination lines via some geometrical models. As the refractive indices are sensitive to the temperature and wavelength, by changing either of them, α_{eg} is changed and so is effective geometry [16]. In the present work, we investigate the temperature and wavelength variation of effective geometry parameter by means of the modified four-parameter model and Cauchy equations, respectively. In addition, we also discuss the order parameter dependence of effective geometry parameter.

Order parameter is the most important parameter of LCs, which controls almost all its physical properties. According to Gennes [1], any anisotropic property can be a measure of macroscopic order parameter in the nematic phase. Here, the refractive indices data have been used for the determination of order parameter. Over the years, different methods, either excluding or including the effect of internal fields, have been proposed for the evaluation of order parameter. The order parameter results obtained via different anisotropy properties and following different methods, differ among themselves [17–20]. In this article, we have opted three different approaches for the evaluation of order parameter, which include the methods given by Kuczynski [21] (which is purely based on birefringence data), Vuks [22], and Neugebauer [23]. The modified four-parameter model is applied to fit the experimental data of order parameter obtained using all three methods.

2. Experimental Data

To obtain the fitting results, the refractive indices data of four NLC compounds (1) *p*(*p*-ethoxyphenylazo) phenyl heptanoate, (2) anisylidene-*p*-aminophenyl butyrate, (3) PCH-5, and (4) I52 have been taken from literature [24, 25]. Temperature-dependent refractive indices of *p*(*p*-ethoxyphenylazo) phenyl heptanoate and anisylidene-*p*-aminophenyl butyrate were obtained at 5893 Å. Experimental data of wavelength-dependent refractive indices of PCH-5 and I52 were measured in the visible wavelength range $\lambda = 436$, 508, 546, 589, and 633 nm at $T = 25^{\circ}$C. Nematic-isotropic transition temperatures of *p*(*p*-ethoxyphenylazo) phenyl heptanoate, anisylidene-*p*-aminophenyl butyrate, PCH-5, and I52 were reported as 119.0, 113.0, 54.9, and 103.4°C, respectively.

3. Theory

3.1. Temperature Effect: Modified Four-Parameter Model

Uniaxial liquid crystals are characterized by two main indices of refraction: the ordinary (n_o) and extraordinary (n_e). In our earlier work, we proposed a modified four-parameter model [11] that describes the temperature dependence of ordinary and extraordinary refractive indices. According to it, the temperature effect on NLC refractive indices can be explained in terms of the square root of $\langle n^2 \rangle$ and birefringence (Δn):

$$n_e = \sqrt{\langle n^2 \rangle} + \frac{2}{3}\Delta n, \tag{1}$$

$$n_o = \sqrt{\langle n^2 \rangle} - \frac{1}{3}\Delta n, \tag{2}$$

where $\langle n^2 \rangle$ is defined as $\langle n^2 \rangle = (n_e^2 + 2n_o^2)/3$. On the basis of the available experimental data of n_e and n_o and our fitting results, $\sqrt{\langle n^2 \rangle}$ linearly decreases with increasing temperature, so it can be written as:

$$\sqrt{\langle n^2 \rangle} = A + BT, \tag{3}$$

where $B < 0$.

To describe the temperature dependence of birefringence, Haller's approximation [26] is commonly used. This is given as:

$$\Delta n = (\Delta n)_o \left(1 - \frac{T}{T_c}\right)^{\beta}, \tag{4}$$

where $(\Delta n)_o$ is the extrapolated value of birefringence in the crystalline state (or at $T = 0K$), T_c is the clearing temperature of NLC material under investigation, and exponent β is a material constant.

By substituting the values of $\sqrt{\langle n^2 \rangle}$ and Δn from Eqs. (3) and (4) back into Eqs. (1) and (2), the modified four-parameter model [11] is obtained.

$$n_e(T) = A + BT + \frac{2}{3}(\Delta n)_o \left(1 - \frac{T}{T_c}\right)^{\beta} \tag{5}$$

$$n_o(T) = A + BT - \frac{1}{3}(\Delta n)_o \left(1 - \frac{T}{T_c}\right)^{\beta} \tag{6}$$

This model explains the temperature dependence of NLC refractive indices. Equations (5) and (6) have four unknown parameters A, B, $(\Delta n)_o$, and β. The procedure for the calculation of these parameters is explained in section 4.

3.2. Wavelength Effect: Cauchy Equations

There are few discrete wavelengths for which the experimental data of LC refractive indices is available. Some empirical models permit us to estimate the refractive indices at any wavelength in a given spectral range. Li et al. [10] have modeled the wavelength

dispersion of ordinary and extraordinary refractive indices as:

$$n_e(\lambda) = A_e + \frac{B_e}{\lambda^2} + \frac{C_e}{\lambda^4}, \tag{7}$$

$$n_o(\lambda) = A_o + \frac{B_o}{\lambda^2} + \frac{C_o}{\lambda^4}, \tag{8}$$

where $A_{e,o}$, $B_{e,o}$, and $C_{e,o}$ are Cauchy coefficients and λ is the wavelength of light. These coefficients can be determined if the LC refractive indices at three different wavelengths are known. Like the refractive indices, birefringence also shows dispersion. From Eqs. (7) and (8), the dispersion of birefringence can be expressed as:

$$\Delta n(\lambda) = A_b + \frac{B_b}{\lambda^2} + \frac{C_b}{\lambda^4}, \tag{9}$$

where $A_b = (A_e - A_o)$, $B_b = (B_e - B_o)$, and $C_b = C_e - C_o$.

3.3. Order Parameter

The anisotropy in any physical property is a direct measure of order parameter. In our first approach to obtain the order parameter, a method purely based on birefringence data is used. Kuczynski et al. [21] proposed a simple procedure for the determination of order parameter, directly from the birefringence data, without considering the local field experienced by the liquid crystalline compounds. According to this method, the order parameter is given as:

$$S_{Kucz} = \frac{\Delta n}{(\Delta n)_o} \tag{10}$$

In the second approach, first applied to liquid crystals by Chandrasekhar and Madhusudana [26], the order parameter is obtained by using the Vuks isotropic field hypothesis [22]. The Vuks assumption leads to the following result:

$$S_{Vuks}\left(\frac{\Delta\alpha}{\alpha}\right) = \frac{n_e^2 - n_o^2}{\langle n^2\rangle}, \tag{11}$$

where $\Delta\alpha$ denotes the anisotropy of molecular polarizability and α is the mean polarizability. The value of $(\Delta\alpha/\alpha)$ can be found by using Haller's [27] extrapolation method. To find out the value of $(\Delta\alpha/\alpha)$, the term $\log((n_e^2 - n_o^2)/\langle n^2\rangle)$ is plotted against $\log(1 - T/T_c)$. This plot comes out to be linear and can be extrapolated to $T = 0$ K. The intercept at $T = 0$ K, where the complete ordering occurs, gives the value of $(\Delta\alpha/\alpha)$. Substituting the value of this factor back in to Eq. (11), the order parameter can be obtained.

In the third approach, following Neugebauer method [23], the order parameter is given by:

$$S_{Neug}\left(\frac{\Delta\alpha}{\alpha}\right) = G(B), \tag{12}$$

where $G(B) = \frac{9}{4B}\left[\left(B^2 - \left(\frac{10}{3}B\right) + 1\right)^{1/2} + \frac{B}{3} - 1\right]$ and $B = \frac{\langle n^2\rangle - 1}{\langle n^2\rangle + 1}\left(\frac{n_e^2+2}{n_e^2-1} + 2\frac{n_o^2+2}{n_o^2-1}\right)$.

The value of $(\Delta\alpha/\alpha)$ is obtained by plotting a log–log plot between $G(B)$ and $(1 - T/T_c)$. Following the extrapolation technique adopted in the previous method, we can obtain the order parameter.

Table 1. Fitting parameters for the modified four-parameter model

	$\sqrt{\langle n^2 \rangle}$		(Δn)	
LC material	A	B (T^{-1})	$(\Delta n)_o$	β
p(*p*-ethoxyphenylazo) phenyl heptanoate	1.6419	-5.39×10^{-4}	0.3498	0.1977
anisylidene-*p*-aminophenyl butyrate	1.6407	-5.44×10^{-4}	0.3071	0.2404

4. Results and Discussion

The modified four-parameter model, Eqs. (5) and (6), contains four unknown parameters. These four parameters are obtained by fitting the temperature-dependent experimental data of $\sqrt{\langle n^2 \rangle}$ and Δn. A linear fitting curve that illustrates the temperature dependence of $\sqrt{\langle n^2 \rangle}$, Eq. (3), gives the value of A and B. While, the fitting of the experimental data of Δn, Eq. (4) in logarithmic form, gives the value of $(\Delta n)_o$ and β. Table 1 contains these four fitting parameters for *p*(*p*-ethoxyphenylazo) phenyl heptanoate and anisylidene-*p*-aminophenyl butyrate. By substituting these parameters into Eqs. (5) and (6), we can compute the temperature dependence of ordinary and extraordinary refractive indices of NLCs.

Figure 1 illustrates the variation of ordinary and extraordinary refractive indices with temperature (T/T_c) for *p*(*p*-ethoxyphenylazo) phenyl heptanoate and anisylidene-*p*-aminophenyl butyrate. Triangles and stars represent the experimental data of refractive indices for *p*(*p*-ethoxyphenylazo) phenyl heptanoate and anisylidene-*p*-aminophenyl butyrate, respectively. The solid lines are the fitting results obtained by the application of

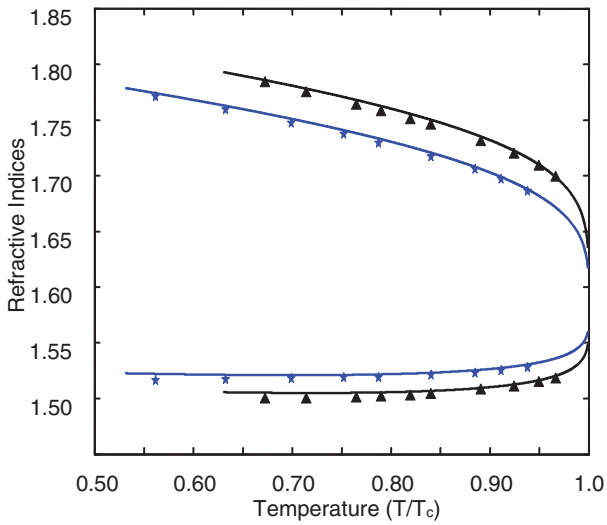

Figure 1. Temperature dependence of refractive indices (n_e, n_o). Experimental data is presented as triangles for *p*(*p*-ethoxyphenylazo) phenyl heptanoate and stars for anisylidene-*p*-aminophenyl butyrate. Corresponding solid lines are the fitting results of four-parameter model (Eqs. (5) and (6)).

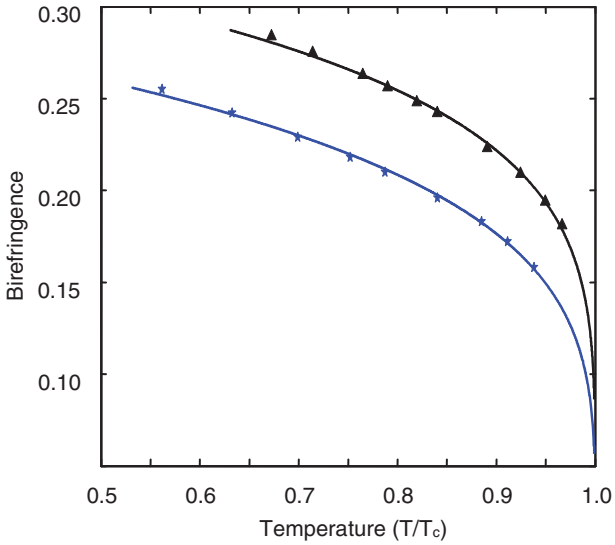

Figure 2. Temperature dependence of birefringence (Δn). Experimental data is presented as triangles for *p*(*p*-ethoxyphenylazo) phenyl heptanoate and stars for anisylidene-*p*-aminophenyl butyrate. Corresponding solid lines are the fitting results of Eq. (4).

modified four-parameter model, Eqs. (5) and (6). With increasing temperature, the refractive indices (n_e, and n_o) show different behavior. The extraordinary refractive index (n_e) strongly depends on the temperature and decreases, in the whole nematic range, with an increase in temperature. While the ordinary refractive index (n_o) shows a weak temperature dependence in the beginning but increases gradually near the clearing temperature. As seen in Fig. 1, the modified four-parameter model fits the experimental data very well, during the whole nematic range, for both NLC materials. Thus, it is an appropriate model to describe the temperature dependence of NLC refractive indices. The temperature dependence of optical birefringence is shown in Fig. 2. Triangles and stars represent the experimental data of birefringence (Δn) for *p*(*p*-ethoxyphenylazo) phenyl heptanoate and anisylidene-*p*-aminophenyl butyrate, respectively. The solid lines are the fitting results obtained from Eq. (4). The birefringence decreases with increasing temperature and the temperature dependence is strong in the neighborhood of nematic-isotropic transition region. Fitting results are found consistent with the experimental data points.

Variation of effective geometry parameter (α_{eg}) as a function of temperature (T/T_c) is depicted in Fig. 3. Triangles and stars represent the temperature-dependent experimental data of α_{eg} for *p*(*p*-ethoxyphenylazo) phenyl heptanoate and anisylidene-*p*-aminophenyl butyrate, respectively. Solid lines are the fitting results obtained by using the four-parameter model, the ratio of Eqs. (5) and (6). The agreement between the experimental data of $\alpha_{eg}(T)$ and our fitting results is quite well. It is observed that α_{eg} slightly increases with an increase in temperature and reaches unity as the operating temperature approaches the transition temperature. Anisylidene-*p*-aminophenyl butyrate has a higher value of α_{eg} as compared to *p*(*p*-ethoxyphenylazo) phenyl heptanoate. According to Sastry et al. [28], the LC material owning higher value of α_{eg} exhibits a lower deflection of light; it is attributed to the lower orientation of director field. Accordingly, anisylidene-*p*-aminophenyl butyrate will exhibit a lower deflection of light than the *p*(*p*-ethoxyphenylazo) phenyl heptanoate.

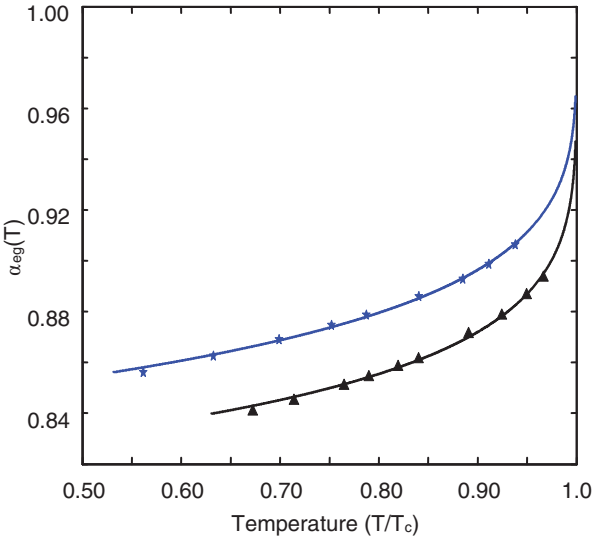

Figure 3. Temperature dependence of effective geometry parameter (α_{eg}). Experimental data is presented as triangles for *p*(*p*-ethoxyphenylazo) phenyl heptanoate and stars for anisylidene-*p*-aminophenyl butyrate. Corresponding solid lines are the fitting results using four-parameter model (Eqs. (5) and (6)).

Equations (7) and (8) have six Cauchy coefficients [A_e, B_e, C_e] and [A_o, B_o, C_o] for n_e and n_o, respectively. These coefficients have been obtained from the experimentally known values of n_e and n_o at three different wavelengths. Values of these coefficients, for two LC materials PCH-5 and I52, are listed in Table 2. Figures 4 and 5 depict the wavelength-dependent refractive indices (n_e, n_o) and birefringence (Δn), respectively. Circles and squares represent the experimental data for PCH-5 and I52, respectively. Fitting curves for the dispersion of $n_e(\lambda)$, $n_o(\lambda)$, and $\Delta n(\lambda)$ were obtained by using Eqs. (7), (8), and (9), respectively. A fine agreement is obtained between the experimental data points and the fitting results. It can be seen that the dispersion of refractive indices is normal, meaning that they decrease with increasing wavelength. The dispersion of n_e is clearly greater than that of n_o. The wavelength dependence of α_{eg} is shown in Fig. 6. Circles and squares represent the experimental data of $\alpha_{eg}(\lambda)$ for PCH-5 and I52, respectively. The fitting curves are obtained by using the Eqs. (7) and (8). The fitting results are in well agreement with the experimental data of $\alpha_{eg}(\lambda)$. PCH-5, having a higher value of α_{eg} as compared to I52, will exhibit a lower deflection of light. Satiro and Moraes [15] have observed the similar nature of α_{eg} as a function of temperature and wavelength.

Table 2. Fitting parameters for the Cauchy model

	n_e			n_o		
LC material	A_e	B_e (λ^{-2})	C_e (λ^{-4})	A_o	B_o (λ^{-2})	C_o (λ^{-4})
PCH-5	1.6076	−0.6107	23.5929	1.4892	−0.3165	11.2865
I52	1.6165	0.7650	9.8756	1.4930	0.1537	6.3761

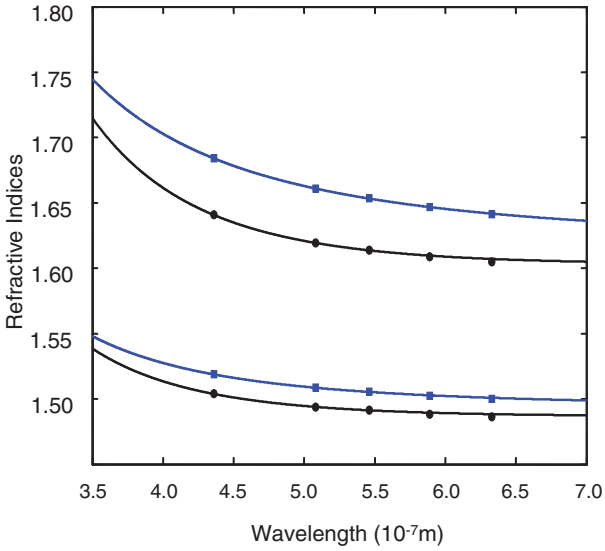

Figure 4. Wavelength dependence of refractive indices (n_e, n_o). Experimental data is presented as circles for PCH-5 and squares for I52. Corresponding solid lines are the fitting results of Cauchy equations (Eqs. (7) and (8)).

The comparison of order parameter obtained in different ways is presented in Figs. 7 and 8 for compounds *p*(*p*-ethoxyphenylazo) phenyl heptanoate and anisylidene-*p*-aminophenyl butyrate, respectively. Circles, squares, and triangles represent the experimental data points for the birefringence, Vuks, and Neugebauer methods, respectively. Solid lines represent the

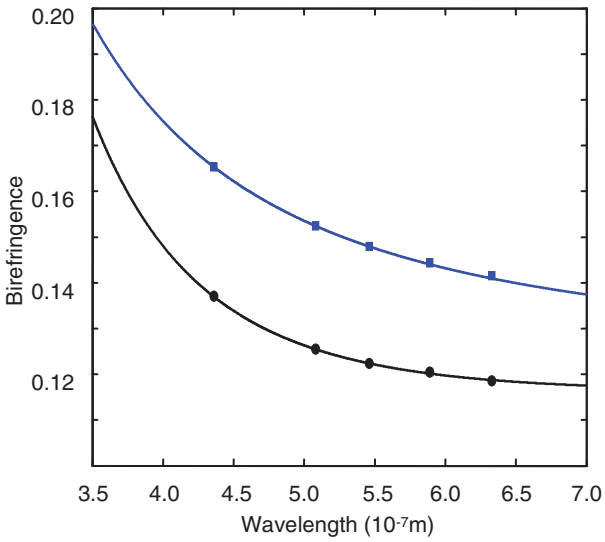

Figure 5. Wavelength dependence of birefringence (Δn). Experimental data is presented as circles for PCH-5 and squares for I52. Corresponding solid lines are the fitting results of Eq. (9).

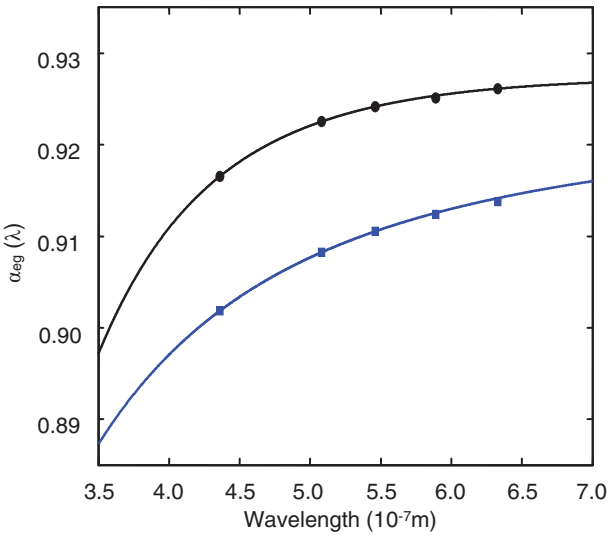

Figure 6. Wavelength dependence of effective geometry parameter (α_{eg}). Experimental data is presented as circles for PCH-5 and squares for I52. Corresponding solid lines are the fitting results using Cauchy equations (Eqs. (7) and (8)).

fitting results obtained by using Eqs. (10), (11), and (12). A very good agreement between the experimental data and fitting curves is found for all three methods. It is suggested by many studies that the results of order parameter obtained from different methods may differ. In the present study also, there is a divergence in the values of order parameter

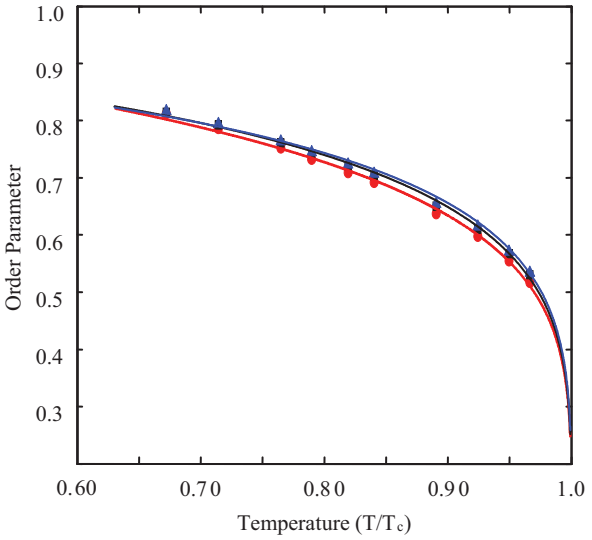

Figure 7. Temperature dependence of order parameter for *p*(*p*-ethoxyphenylazo) phenyl heptanoate. Experimental data is presented as circles for birefringence, squares for Vuks, and triangles for Neugebauer methods. Corresponding Solid lines are the fitting results of Eqs. (10), (11), and (12).

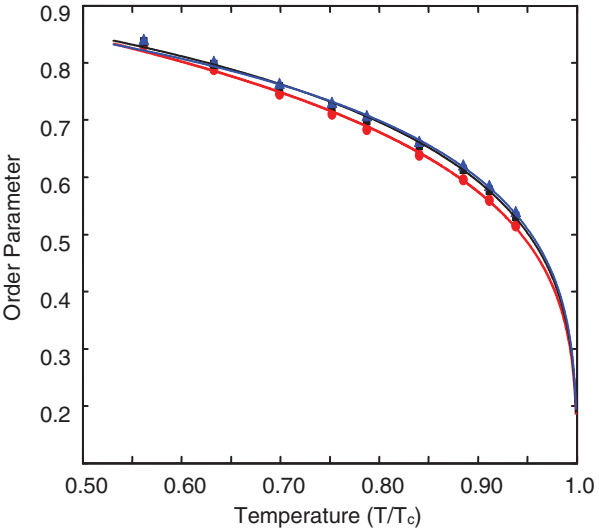

Figure 8. Temperature dependence of order parameter for anisylidene-*p*-aminophenyl butyrate. Experimental data is presented as circles for birefringence, squares for Vuks, and triangles for Neugebauer methods. Corresponding Solid lines are the fitting results of Eqs. (10), (11), and (12).

from one method to another. The order parameter obtained from Neugebauer approach is found to be slightly higher than the one obtained by Vuks method. The deviation between Neugebauer and Vuks approaches varies only from 0.26% at $T = 0.67T_c$ to 0.73% at $T = 0.96T_c$ for *p*(*p*-ethoxyphenylazo) phenyl heptanoate and from 0.26% at $T = 0.56T_c$ to

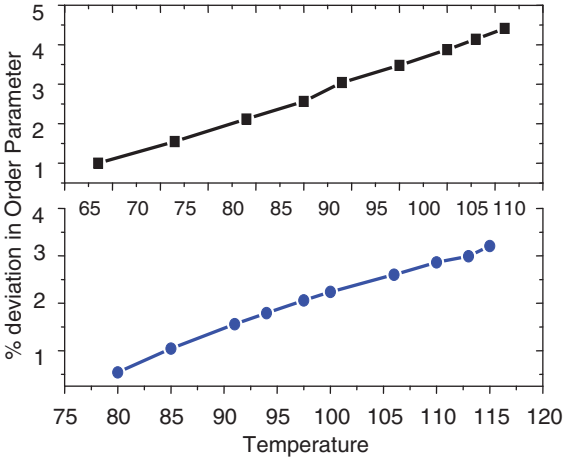

Figure 9. Temperature dependence of percentage deviation in order parameter between Neugebauer and birefringence methods. Squares and circles represent the order parameter deviation for anisylidene-*p*-aminophenyl butyrate and for *p*(*p*-ethoxyphenylazo) phenyl heptanoate, respectively.

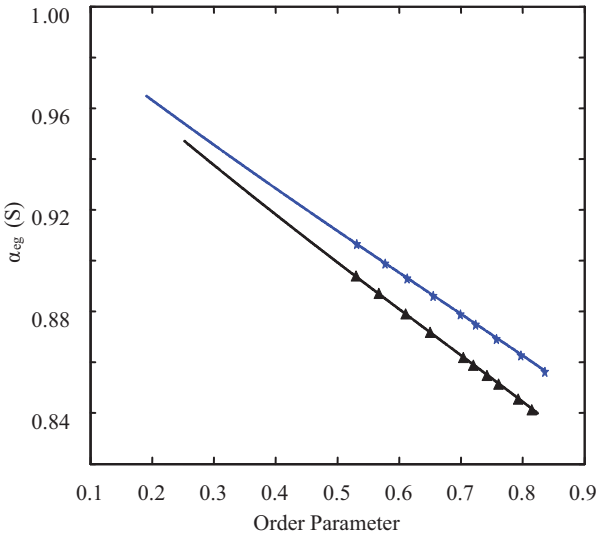

Figure 10. Order parameter dependence of effective geometry parameter (α_{eg}). Experimental data is presented as triangles for *p*(*p*-ethoxyphenylazo) phenyl heptanoate and stars for anisylidene-*p*-aminophenyl butyrate. Corresponding solid lines are the fitting curves of α_{eg} against Eq. (11).

1.07% at $T = 0.93T_{\mathrm{c}}$ for anisylidene-*p*-aminophenyl butyrate. The noticeable differences are observed while using the birefringence method. Order parameter obtained by using the birefringence method is found to be lower than the ones obtained from the Vuks and Neugebauer methods. The difference between order parameter values obtained by birefringence and Neugebauer is found from 0.54% at $T = 0.67T_{\mathrm{c}}$ to 3.20% at $T = 0.96T_{\mathrm{c}}$ for *p*(*p*-ethoxyphenylazo) phenyl heptanoate and from 0.99% at $T = 0.56T_{\mathrm{c}}$ to 4.41% at $T = 0.93T_{\mathrm{c}}$ for anisylidene-*p*-aminophenyl butyrate. The deviations among the order parameter values are more pronounced near the transition temperature. In Fig. 9, the percentage deviation between Neugebauer and birefringence methods is plotted. With increasing temperature, a continuous increase in the deviation of order parameter results is observed.

Figure 10 depicts the order parameter dependence of effective geometry parameter, $\alpha_{eg}(S)$. Triangles and stars represent the experimental data of $\alpha_{eg}(S)$ for *p*(*p*-ethoxyphenylazo) phenyl heptanoate and anisylidene-*p*-aminophenyl butyrate, respectively. Solid lines are the fitting results of $\alpha_{eg}(S)$, obtained by using the four-parameter model. Experimental data and fitting results of order parameter used for this plot are obtained via Vuks method (Eq. (11)). In Fig. 10, it can be seen that α_{eg} linearly decreases as the ordering of the LC molecules increases. When the value of α_{eg} reaches unity, there is no more ordering in liquid crystals. The corresponding temperature at this point ($\alpha_{eg} = 1$) indicates the isotropic state. Recently, some other authors have also experimentally studied the temperature and order parameter dependence of effective geometry parameter [29, 30]. Satiro and Moraes [15, 16, 31] have also investigated the temperature and wavelength effect on α_{eg} and the effect of the variation of this ratio on the deflection of light in liquid crystals. Our results are consistent with those obtained in references [15, 16, 29–31].

5. Conclusions

The four-parameter model and the Cauchy model, describing the temperature and wavelength dependence of NLC refractive indices, are confirmed by the experimental data. Experimental data of four different NLC systems are used to validate these models. The models used to explain the temperature and wavelength effect on NLC refractive indices for a particular set of data could be applicable in general for the other NLC compounds. Temperature and wavelength dependency of effective geometry parameter is also well described by these models. The four-parameter model forms a theoretical tool to analyze the experimental data of liquid crystalline systems involving the refractive indices and the order parameter obtained from refractive indices. The degree of light deflection in nematics is identified with the numerical value of effective geometry parameter. The empirical models used in this article can be incorporated with some geometrical models [15, 16], describing the propagation of light around topological defects in NLCs, in order to study the effect of temperature and wavelength.

References

[1] De Gennes, P. G. et al. (1993). *The Physics of Liquid Crystals*, Oxford University Press: New York.
[2] Collings, P. J. et al. (1997). *Introduction to Liquid Crystals: Chemistry and Physics*, Taylor and Francis: London.
[3] Pelzl, G. (1998). Optical Properties of Nematic Liquid Crystals. In: D. Demus, J. Goodby, G. W. Gray, H. W. Spiess, & V. Vill (Eds.), *Handbook of Liquid Crystals,* Vol. 2A, Wiley-VCH: Weinheim, p. 128.
[4] Hirschmann, H. et al. (1998). Applications: TN, STN Displays. In: D. Demus, J. Goodby, G. W. Gray, H. W. Spiess, & V. Vill (Eds.), *Handbook of Liquid Crystals*, Wiley-VCH: Weinheim, p. 199.
[5] Li, J., & Wu, S. T. (2004). *J. Appl. Phys.*, *96*, 170.
[6] Wu, S. T. (1986). *Phys. Rev. A*, *33*, 1270.
[7] Abdulhalim, I. (1991). *Mol. Cryst. Liq. Cryst.*, *197*, 103.
[8] Averynov, E. M. (1997). *J. Opt. Tech.*, *64*, 471.
[9] Li, J., Gauza, S., & Wu, S. T. (2004). *J. Appl. Phys.*, *96*, 19.
[10] Li, J., & Wu, S. T. (2004). *J. Appl. Phys.*, *95*, 896.
[11] Soorya, T. N., Gupta, S., Kumar, A., Jain, S., Arora, V. P., & Bahadur, B. (2006). *Ind. J. Pure Appl. Phys.*, *44*, 524.
[12] Brandenberger, R. H. (1998). *Pramana J. Phys.*, *51*, 191.
[13] Ambrozic, M., Kralj, S., & Virga, E. G. (2007). *Phys. Rev. E*, *75*, 031708.
[14] Repnik, R., Mathelitsch, L., Svetec, M., & Kralj, S. (2003). *Eur. J. Phys.*, *24*, 481.
[15] Satiro, C., & Moraes, F. (2008). *Eur. Phys. J. E*, *25*, 425.
[16] Satiro, C., & Moraes, F. (2009). *Mol. Cryst. Liq. Cryst.*, *508*, 261.
[17] Das, M. K., Sarkar, G., Das, B., Rai, R., & Sinha, N. (2012). *J. Phys.: Condens. Matter*, *24*, 11510.
[18] Horn, R. G. (1978). *J. Phys. France*, *39*, 105.
[19] Zywucki, B. J., & Kuczynski, W. (2001). *IEEE Transactions on Dielectrics and Electrical Insulation*, *8*, 512.
[20] Kumar, A. (2007). *Acta Physica. Polonica. A*, *112*, 1213.
[21] Kuczynski, W., Zywucki, B., & Malecki, J. (2002). *Mol. Cryst. Liq. Cryst.*, *381*, 1.
[22] Vuks, M. F. (1966). *Opt. Spektrosk.*, *20*, 644.
[23] Neugebauer, H. E. J. (1954). *Can. J. Phys.*, *32*, 1.
[24] Finkenzeller, U., Geelhaar, T., Weber, G., & Pohl, L. (1989). *Liq. Cryst.*, *5*, 313.

[25] Somashekar, R., Revannasiddaiah, D., Madhava, M. S., Subramhanyam, H. S., & Krishnamurti, D. (1978). *Mol. Cryst. Liq. Cryst.*, *45*, 243.
[26] Chandrasekhar, S., & Madhusudana, N. V. (1969). *J. Physique Colloq.*, *30*, C4–24.
[27] Haller, I. (1975). *Prog. Solid State Chem.*, *10*, 103.
[28] Sastry, S. S., Kumari, T. V., Begum, S. S., & Rao, V. V. (2011). *Liq. Cryst.*, *38*, 277.
[29] Sastry, S. S., Kumari, T. V., Mallika, K., Rao, B. G. S., Ha, S. T., & Lakshminarayana, S. (2012). *Liq. Cryst.*, *39*, 295.
[30] Pisipati, V. G. K. M., Latha, D. M., Prasad, P. V. D., & Rani, G. P. (2012). *J. Mol. Liq.*, *174*, 1.
[31] Satiro, C., & Moraes, F. (2006). *Eur. Phys. J. E*, *20*, 173.